

Received: 21 June 2007,

Revised: 23 August 2007,

Accepted: 20 September 2007,

Published online in Wiley InterScience: 4 December 2007

(www.interscience.wiley.com) DOI 10.1002/poc.1284

A DFT study of transition structures and reactivity in solvolyses of *tert*-butyl chloride, cumyl chlorides, and benzyl chlorides

Ferenc Ruff^a* and Ödön Farkas^a



DFT computations were performed on the S_N1 and S_N2 solvolyses of substituted cumyl chlorides and benzyl chlorides in ethanol and water, by increasing stepwise the C—Cl distance and by optimization. The total energy increases with the increase in the Cl—C distance in S_N1 reactions, while free energy of activation pass through maximum. To validate the results, the calculated free energies of activation were compared with data obtained by kinetic measurements. The structural parameters of the transition states were correlated with the Hammett substituent constants and compared with the data of hydrolyses of *tert*-butyl chloride and methyl chloride, which proceed with known mechanisms. Conclusions on the mechanisms of the reactions were driven from the effect of substituents on free energies of activation. Cumyl chlorides substituted with electron-donating (e-d) groups solvolyze with S_N1 mechanism, while the reactions of substrates that bear electron-withdrawing groups proceed with weak nucleophilic assistance of the solvent. Benzyl chlorides hydrolyze through an S_N2 pathway except those derivatives that have strongly e-d groups, where the reaction has S_N1 character, but a weak nucleophilic assistance of the water should also be taken into consideration. Copyright © 2007 John Wiley & Sons, Ltd.

Supplementary electronic material for this paper is available in Wiley InterScience at <http://www.mrw.interscience.wiley.com/suppmat/0894-3230/suppmat/>

Keywords: nucleophilic substitutions; *tert*-butyl chloride; cumyl chlorides; benzyl chlorides; substituent effect; activation parameters; DFT calculations

INTRODUCTION

The mechanism of aliphatic nucleophilic substitutions has been thoroughly investigated.^[1] S_N1 reactions proceed with rate-determining formation of intimate and/or solvent separated ion pairs,^[2] while concerted S_N2 reactions proceed with the synchronous formation and splitting of bonds of the nucleophile and the leaving group,^[1,3] respectively. In S_N1 reactions of adamantly halides,^[3a] the nucleophile does not take part in the rate-determining step because of steric hindrance. Nevertheless, in other cases the rate-determining heterolysis and the amount of nucleophilic solvent assistance depend on electronic and steric effects of substituents.^[3] Bentley and Schleyer^[3a] designated the mechanisms which involve nucleophilically solvated ion pair intermediates by the term S_N2 (intermediate). Gajewski explained,^[4] however, reactivity in nucleophilic substitution reactions by hydrogen bond donation to the leaving group, rather than by the nucleophilic solvent participation.

Earlier we made DFT computations^[5] on the effect of substituents on activation parameters and transition structures of S_N2 reactions. Free energy, enthalpy and entropy of activation data were correlated with the Hammett σ constants^[5,6] (Eqn 1, $P = G, H$, or S).

$$\Delta P^\ddagger = \delta \Delta P^\ddagger \sigma + \Delta P_0^\ddagger \quad (1)$$

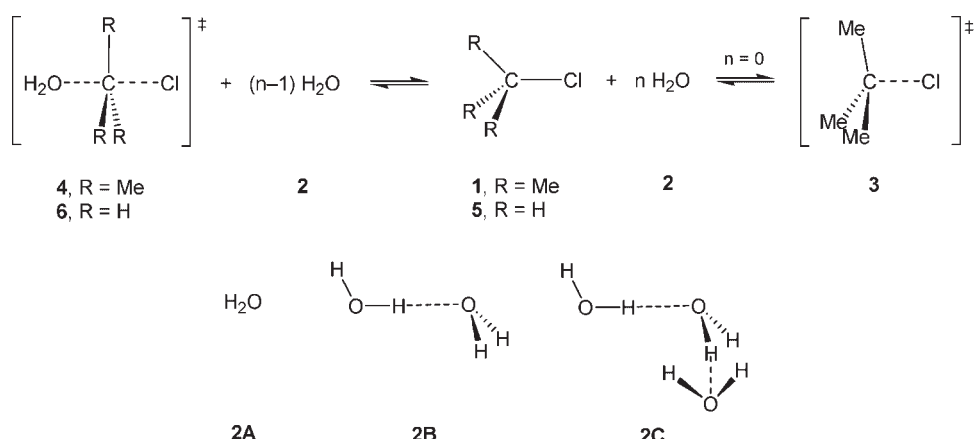
ΔP^\ddagger and ΔP_0^\ddagger are the activation parameters of the substituted and unsubstituted compounds, respectively. The $\delta \Delta P^\ddagger$ reaction constants are the changes in the activation parameters per unit

change in the σ substituent constants. By using Heppeler's theory^[7] we have shown^[5] that in S_N2 reactions the rearrangement of the solvent molecules influences mainly the values of the experimentally determined entropy and enthalpy of activation. These parameters, however, decrease/increase together with the increase/decrease in solvation, and their changes approximately cancel each other, according to equation $\delta \Delta G^\ddagger = \delta \Delta H^\ddagger - T \delta \Delta S^\ddagger \approx 0$. Therefore, the ΔG^\ddagger values, obtained by DFT calculations approximate well the experimental data for S_N2 reactions. The effect of solvent polarity on reactivity (on ΔG^\ddagger) can be computed with the polarizable continuum model (PCM) of solvents implemented in the Gaussian program package.^[5] The use of the PCM solvent model means that calculations are carried out in a polarizable, continuous medium of the same dielectric constant as the solvent. On the other hand, calculated and experimental ΔH^\ddagger and ΔS^\ddagger data may deviate from each other because the rearrangements of the solvent molecules, which proceed during the reactions, are not taken into account with the applied computational methods.

To test the methods of calculations in S_N1 reactions, and to study the change of mechanism and reactivity with substituents

* Department of Organic Chemistry, Institute of Chemistry, L. Eötvös University, P. O. Box 32, H-1518 Budapest 112, Hungary.
E-mail: ruff@chem.elte.hu

a F. Ruff, Ö. Farkas
Department of Organic Chemistry, Institute of Chemistry, L. Eötvös University, H-1518 Budapest 112, Hungary

Scheme 1. Hydrolysis of *tert*-butyl chloride (1) and methyl chloride (5)

in aliphatic nucleophilic substitutions we made DFT computations on the solvolyses of cumyl chlorides and benzyl chlorides. The first reaction has been accepted to be an S_N1 processes, the mechanism of the latter one was thought to change with the substituents of the benzene ring.^[1] To validate the method of computations the widely investigated hydrolyses of *tert*-butyl chloride and methyl chloride have also been studied.

RESULTS AND DISCUSSIONS

Hydrolysis of *tert*-butyl chloride and methyl chloride

tert-butyl chloride (1) is thought to hydrolyze with an S_N1 mechanism^[1a,f,2b,4,8] (Scheme 1, $1 \rightleftharpoons \text{TS } 3$), though evidences have also been presented^[3d,9,10] that the reaction proceeds with nucleophilic assistance of the solvent [S_N2 (intermediate) mechanism, Scheme 1, $1 + 2\text{A} \rightleftharpoons \text{TS } 4$]. We made calculations on this reaction at DFT(B3LYP)/6-31G(d) level. Selected structural data and thermochemical parameters, computed for both mechanisms can be found in Tables 1 and 2, moreover in Tables S1 and S5 in the Supplementary Materials.

In the S_N1 reaction the total energy (E) of the *tert*-butyl chloride species increases continuously with the increase in the C—Cl bond, therefore, locating corresponding TS on the potential energy surface is impossible. However, free energy has a maximum along the reaction path and can be used to identify the transition state (TS). Free energy (G), enthalpy (H), and entropy (S) values for finding the appropriate structure for TS 3 were computed via relaxed scan applied on the C—Cl distance. The ΔE^\ddagger , ΔG^\ddagger , ΔH^\ddagger , and ΔS^\ddagger activation parameters were calculated from the differences of the E , G , H , and S values of the scan points and reactant 1. ΔG^\ddagger data have a maximum value at $R(\text{ClC}) = 3.25 \text{ \AA}$, other activation parameters increase continuously with the increase in the C—Cl distance (Fig. 1). The structure with maximum value of ΔG^\ddagger is regarded as the TS of the S_N1 process. TS 3 has one imaginary frequency, which corresponds to the splitting of the C—Cl bond. Weak interaction occurs between the Cl and *t*-Bu moieties in TS 3, the charge of chlorine is less than unity, the *tert*-butyl group shows slight deviation from coplanar arrangement (Table 1). $\Delta G^\ddagger = 90.1 \text{ kJ mol}^{-1}$ was computed for the formation of TS 3, while $\Delta G^\ddagger = 81.8 \text{ kJ mol}^{-1}$ was obtained from the measured first-order rate constant^[11] in water, at 298 K (Table 2).

Table 1. Charges (Q , a.u.), bond distances (R , \AA), and bond angles (θ , degree) of the TSs of hydrolyses of *tert*-butyl chloride (TSs 3 and 4), methyl chloride (TS 6), cumyl chlorides (TSs 8 and 9), and benzyl chlorides (TSs 11 and 12), calculated at (B3LYP)/6-31G(d) level, in water (for 3, 4, 6, 11, and 12) and ethanol (for 8 and 9), at 298 K

| TS | X | $Q(\text{Cl})$ | $Q(\text{O})$ | $R(\text{ClC})$ | $R(\text{OC})$ | $\theta(\text{CICO})$ | $\theta(\text{CICR})^a$ | $\theta(\text{CICC}^\dagger)$ |
|-----|-------------------|----------------|---------------|-----------------|----------------|-----------------------|-------------------------|-------------------------------|
| 3 | — | -0.889 | — | 3.25 | — | — | 93.2 | — |
| 4 | — | -0.890 | 0.068 | 3.044 | 2.668 | 177.6 | 92.0 | — |
| 6 | — | -0.717 | 0.264 | 2.425 | 1.904 | 177.9 | 86.8 | — |
| 8a | H | -0.934 | — | 3.337 | — | — | 86.7 | 99.0 |
| 8b | 4-MeO | -0.921 | — | 3.165 | — | — | 90.0 | 99.2 |
| 8c | 4-NO ₂ | -0.900 | — | 3.367 | — | — | 88.5 | 100.4 |
| 9a | H | -0.927 | 0.042 | 3.233 | 2.892 | 169.6 | 88.5 | 96.1 |
| 9c | 4-NO ₂ | -0.907 | 0.095 | 3.204 | 2.479 | 178.5 | 88.2 | 90.0 |
| 11a | H | -0.946 | — | 3.684 | — | — | 75.9 | 117.3 |
| 11b | 4-MeO | -0.929 | — | 3.314 | — | — | 76.7 | 118.9 |
| 11c | 4-NO ₂ | -0.928 | — | 3.889 | — | — | 77.8 | 114.4 |
| 12a | H | -0.821 | 0.215 | 2.699 | 2.049 | 157.6 | 79.0 | 101.6 |
| 12b | 4-MeO | -0.898 | 0.197 | 2.927 | 2.101 | 149.7 | 75.4 | 106.4 |
| 12c | 4-NO ₂ | -0.760 | 0.252 | 2.593 | 1.971 | 164.5 | 80.8 | 97.0 |

^a R = H or Me.

Table 2. Calculated and experimentally derived activation parameters (ΔG^\ddagger , ΔH^\ddagger , ΔS^\ddagger) of the hydrolyses of *tert*-butyl chloride (**1**), methyl chloride (**5**), cumyl chloride (**7a**), and benzyl chloride (**10a**), and effect of substituents on free energy of activation ($\delta\Delta G^\ddagger$) in reactions of substituted compounds

| Reaction | $\Delta G_{\text{calc}}^\ddagger$ ^a | $\Delta G_{\text{exp}}^\ddagger$ ^a | $\delta\Delta G_{\text{calc}}^\ddagger$ ^b | $\delta\Delta G_{\text{exp}}^\ddagger$ ^b | $\Delta H_{\text{calc}}^\ddagger$ ^a | $\Delta H_{\text{exp}}^\ddagger$ ^a | $\Delta S_{\text{calc}}^\ddagger$ ^c | $\Delta S_{\text{exp}}^\ddagger$ ^c |
|--|--|---|--|---|--|---|--|---|
| 1 \rightleftharpoons TS 3 | 90.1 | 81.8 | — | — | 102.8 | 97.2 | 20.4 | 51.0 |
| 1 + 2 \rightleftharpoons TS 4 | 93.1 ^d | 91.8 | — | — | 102.4 | 97.2 | 31.5 | -18.1 |
| 5 + 2 \rightleftharpoons TS 6 | 121.2 | 126.7 | — | — | 80.1 | 111.5 | -138 | -50.9 |
| 7a \rightleftharpoons TS 8a | 52.3 | 92.3 | 33.5 | 28.0 | 63.2 | 79.5 ^e | 36.6 | -54.0 ^e |
| 7a + 2 \rightleftharpoons TS 9a | 59.8 | 99.4 | 36.0 | 28.0 | 71.4 | — | 30.3 | — |
| 10a \rightleftharpoons TS 11a | 99.2 | 101 | 56.2 | 11.8/28.6 ^f | — | — | — | — |
| 10a + 2 \rightleftharpoons TS 12a | 99.9 | 111 | 12.7 | 11.8/28.6 ^f | 60.3 | 85.3 | -131 | -85.3 |

Calculations [at DFT(B3LYP)/6-31G(d) level] and measurements were carried out in water (for **1**, **5**, and **10a**) and in ethanol (for **7a**), at 298 K.

^a In kJ mol^{-1} .

^b In $\text{kJ mol}^{-1} \text{Å}^{-1}$.

^c In $\text{J mol}^{-1} \text{K}^{-1}$.

^d Calculated for the reaction **1** + **2C** \rightleftharpoons TS **4** + **2B**, for the reaction **1** + **2A** \rightleftharpoons TS **4** $\Delta G^\ddagger = 112.6 \text{ kJ mol}^{-1}$ was obtained.

^e Measured in 90% acetone–water.

^f Data for compounds with substituent constants $\sigma^+ \geq 0/\sigma^+ \leq 0$.

The optimized structure of TS **4** of the $\text{S}_{\text{N}}2$ (intermediate) mechanism can be computed with two imaginary frequencies, one of them corresponds to the stretching vibration of the C–Cl bond, the other to the libration of the very weakly bonded water molecule. The bond distances of TS **4** (Table 1) agree well with data [$R(\text{CCl}) = 3.0 \text{ \AA}$, $R(\text{OC}) = 2.6 \text{ \AA}$] calculated by Jorgensen *et al.*^[12] in a detailed study on the hydrated $\text{H}_2\text{O} \cdots t\text{-Bu}^+\text{Cl}^-$ contact ion pair in water. The $R(\text{CCl}) = 3.390 \text{ \AA}$ and $R(\text{OC}) = 1.742 \text{ \AA}$ bond distances calculated by Martinez *et al.*^[13] for TS **4** show great deviations from the former values, and rather due to the complex of chloride ion and protonated *tert*-butanol ($\text{Cl}^- \cdots t\text{BuOH}_2^+$), bonded with Cl–H hydrogen bondings together. Though the calculated $R(\text{CCl})$ distance of TS **4** is somewhat

shorter than that of TS **3**, the structures of the $\text{Cl} \cdots t\text{-Bu}$ moieties are very similar in both TSs (Table 1). On the other hand, in the case of TS **4** the $R(\text{CCl})$ and $R(\text{OC})$ bond distances are much longer, the negative charge of chlorine is greater, the positive charge of the oxygen atom is much smaller than in TS **6**, calculated for the $\text{S}_{\text{N}}2$ hydrolysis of methyl chloride (**5**) (Scheme 1, Table 1). The bond distances calculated for TS **6** agree well with the data $R(\text{CCl}) = 2.500 \text{ \AA}$ and $R(\text{OC}) = 1.975 \text{ \AA}$ obtained by Aida *et al.*^[14] for this structure.

The $\Delta G^\ddagger = 121.2 \text{ kJ mol}^{-1}$ value, computed for the $\text{S}_{\text{N}}2$ hydrolysis of methyl chloride (**5** + **2A** \rightleftharpoons TS **6**) agree well with $\Delta G^\ddagger = 126.7 \text{ kJ mol}^{-1}$ obtained by kinetic measurements^[15] in water, at 298 K (Table 2). In the reaction of *tert*-butyl chloride and one water molecule (**1** + **2A** \rightleftharpoons TS **4**) the $\Delta G^\ddagger = 112.6$ and 91.8 kJ mol^{-1} data, calculated by the DFT method and from the $k_2 = k_1/[\text{H}_2\text{O}]$ rate constants,^[11] respectively, show greater deviation, which may originate from the second imaginary frequency of TS **4**. To improve the results, the thermochemical parameters of the H-bonded associations of two (Scheme 1, **2B**) and three water molecules (**2C**) were also calculated with zero and one imaginary frequency, respectively. The imaginary frequency of **2C** corresponds to the libration of the third water molecule, being only a H-bond acceptor. For the reaction with three water molecules ($n = 3$; **1** + **2C** \rightleftharpoons TS **4** + **2B**) $\Delta G^\ddagger = 93.1 \text{ kJ mol}^{-1}$ was calculated, which is in better agreement with the experimentally derived value (Table 2). In the latter reaction there is a species both on the reactant and the product sides (**2C** and TS **4**) with an imaginary frequency, which due to the libration of a water molecule. The imaginary frequency correction (IFC, refer to details in Section Computational Methods) can be used to decrease errors in computed ΔG^\ddagger data.

Computed structural data refer to weak interaction between the *t*-Bu and the water species in TS **4**. In accordance with the results of former investigations,^[3d,9,10] the calculations also support that the hydrolysis of *tert*-butyl chloride proceeds via $\text{S}_{\text{N}}2$ (intermediate) mechanism with the nucleophilic assistance of water, however, the C–O bond in TS **4** is much

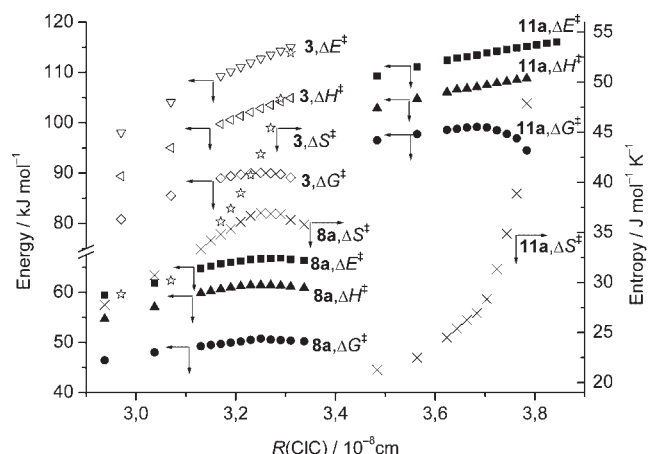
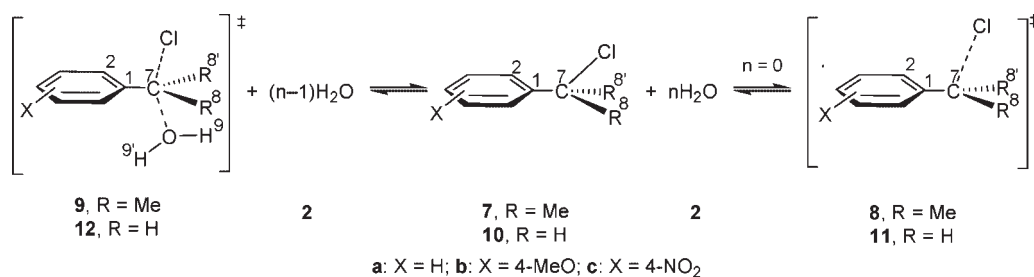


Figure 1. $\Delta E^\ddagger/\Delta G^\ddagger/\Delta H^\ddagger/\Delta S^\ddagger$ versus $R(\text{CIC})$ plots of the formations of TS **3**, **8a**, and **11a** in the $\text{S}_{\text{N}}1$ solvolyses of *tert*-butyl chloride (**1**) cumyl chloride (**7a**), and benzyl chloride (**10a**), respectively. Calculations were performed at (B3LYP)/6-31G(d) level increasing the $R(\text{CIC})$ distance step-wise, in water (for **3** and **11a**) and ethanol (for **8a**), at 298 K



Scheme 2. Hydrolysis of cumyl chlorides (7) and benzyl chlorides (10)

weaker than in TS **6** of the S_N2 hydrolysis of methyl chloride (Table 1).

Solvolution of cumyl chlorides

The nucleophilic substitution reactions on cumyl chlorides (7) are regarded to proceed^[1,16,17] with an S_N1 mechanism (Scheme 2, **7** \rightleftharpoons TS **8**). Rate constants of the hydrolysis of these substrates, measured in 90% acetone–water solvent mixtures, were used to determine^[16] the σ^+ substituent constants. Some authors^[18,19] claimed that the hydrolysis of cumyl derivatives proceeds with the nucleophilic assistance of water (**7** + **2A** \rightleftharpoons TS **9**). On the other hand, Kevil and Dsouza^[20] and Richard *et al.*^[21] have presented evidences using the extended Grunwald–Winstein equation that solvation of these compounds is reduced and becomes insignificant upon increasing internal electron donation.

The optimized structures for reactants and TSs, and the activation parameters for solvolution of cumyl chlorides have been calculated at the DFT(B3LYP)/6-31G(d) level in ethanol. Structural and thermochemical parameters are listed in Tables 1 and 2 moreover in Tables S2 and S6 in the Supplementary Material. The total energy of TS **8a**, and the ΔG^\ddagger , ΔH^\ddagger , and ΔS^\ddagger activation parameters of the S_N1 solvolution (**7a** \rightleftharpoons TS **8a**) pass through maxima, with the increase in the $R(ClC^7)$ distance (Fig. 1). The S_N1 reaction can be calculated therefore both by optimization or by increasing the $R(ClC^7)$ distance stepwise, and $R(ClC^7) = 3.33$ and 3.25 \AA , just as $\Delta G^\ddagger = 49.9$ and 50.8 kJ mol^{-1} were obtained for TS **8a** by these methods, respectively. In this reaction, the total energy and the activation parameters have maximum values, because at $R(ClC^7) > 3.4 \text{ \AA}$, the TS **8a** is transformed to complex of the cumyl cation and the chloride anion [$C_6H_5C(CH_3)_2^+ \cdots Cl^-$], bonded with $CH \cdots Cl$ hydrogen bonding together. The TSs **8**, calculated by both methods have higher energy than the complexes, and have only one imaginary frequency, which corresponds to the splitting of the $Cl \cdots C^7$ bond.

The structures of TSs **9** of the S_N2 (intermediate) mechanism can be calculated by optimization only for the unsubstituted TS **9a** and for those derivatives that have electron-withdrawing (e-w) X substituents. Water is bonded relatively strongly in the TSs **9** of the $X = 4-NO_2$ and $3-NO_2$ derivatives. These TSs have only one imaginary frequency, which leads to the splitting of the $Cl \cdots C^7$ bond and the formation of the $O \cdots C^7$ bond. TSs **9** bearing e-w substituents from $X = 4-CN$ to $X = H$ have a second imaginary frequency, which is the libration of the weakly bonded water molecule. Optimized structures cannot be calculated for TSs **9** of compounds having the electron-donating (e-d) 4-MeO and 4-Me groups.

The structural parameters of the $XC_6H_4(CH_3)_2C \cdots Cl$ moieties of TSs **8** and **9** are similar. The computed charges (Q) and bond distances (R) of the Cl atom depend only slightly on the mechanism of the reactions, and on the electronic effects of the X substituents, and do not give linear correlations with the σ^+ constants (Fig. 2). On the other hand, in TSs **9** the $Q(O)$ positive charge of the oxygen atom of water increases, while the $R(OC^7)$ distance decreases with the increasing σ^+ constant and e-w effect of the X substituent. These parameters display linear correlations with the σ^+ constants (Fig. 2).

The computed and experimentally derived^[16] activation parameters give linear correlations with the σ^+ substituent constants (Fig. 3). To correct the errors originating from the second imaginary frequencies of some TSs **9**, the activation parameters were calculated according to the reactions **7** + **2B** \rightleftharpoons TS **9** + **2A** and **7** + **2C** \rightleftharpoons TS **9** + **2B** for the nitro substituted compounds (with one imaginary frequency), and for other derivatives with weaker e-w groups (with two imaginary frequencies), respectively, using the IFC method. The calculated ΔG^\ddagger values are smaller than the experimental data measured in ethanol. One of the reasons of the differences can be that calculations were performed with the water nucleophile instead of ethanol to promote convergence during geometry optimizations. The slopes, of the computed and experimentally derived ΔG^\ddagger versus σ^+ plots, are similar and depend only slightly on the

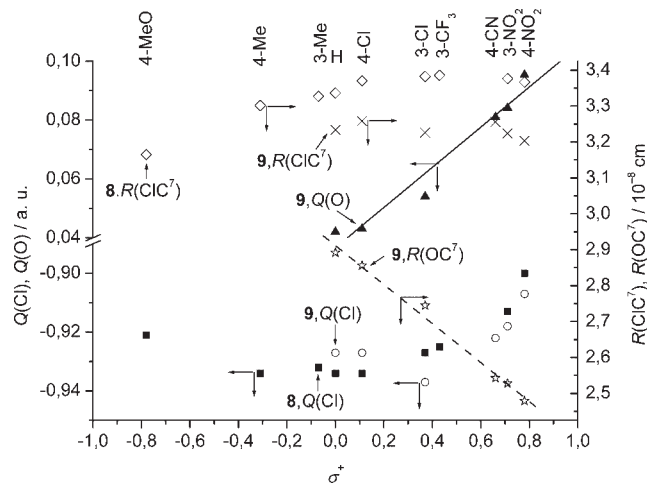


Figure 2. Charges (Q) and bond distances (R) of the TSs of S_N1 (**7** \rightleftharpoons TS **8**, Scheme 2) and S_N2 (**7** + **2A** \rightleftharpoons TS **9**) solvolution of cumyl chlorides (**7**), calculated at (B3LYP)/6-31G(d) level in ethanol, at 298 K. [Correlations for TS **9**: $Q(O) = 0.0683 \sigma^+ + 0.0366$ ($r = 0.976$), $R(OC^7) = -0.543 \sigma^+ + 2.91$ ($r = 0.995$).]

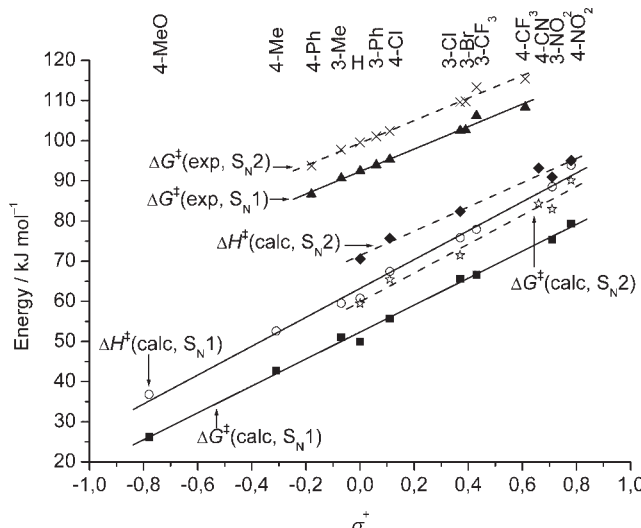


Figure 3. Calculated and experimentally derived^[16] $\Delta G^\ddagger/\Delta H^\ddagger$ versus σ^+ plots of the S_N1 ($7 \rightleftharpoons TS 8$, Scheme 2) and S_N2 ($7 + 2 \rightleftharpoons TS 9$) solvolysis of cumyl chlorides in ethanol, at 298 K. Calculations were performed at (B3LYP)/6-31G(d) level. Experimental data were calculated from the first- and second-order rate constants for S_N1 and S_N2 reactions, respectively. [Correlations for calculated data in ethanol, S_N1 : $\Delta G^\ddagger = 33.5\sigma^+ + 52.3$ ($r = 0.998$), $\Delta H^\ddagger = 36.0\sigma^+ + 63.2$ ($r = 0.996$), $\Delta S^\ddagger = 36.6 \pm 6.0\text{ J mol}^{-1}\text{ K}^{-1}$; S_N2 : $\Delta G^\ddagger = 36.0\sigma^+ + 59.8$ ($r = 0.988$), $\Delta H^\ddagger = 30.2\sigma^+ + 71.4$ ($r = 0.991$), $\Delta S^\ddagger = 30.3 \pm 7.9\text{ J mol}^{-1}\text{ K}^{-1}$. Correlations for experimentally derived data;^[16] ethanol, S_N1 : $\Delta G^\ddagger = 28.0\sigma^+ + 92.3$ ($r = 0.994$); S_N2 : $\Delta G^\ddagger = 28.0\sigma^+ + 99.4$ ($r = 0.994$). Methanol, S_N1 : $\Delta G^\ddagger = 27.5\sigma^+ + 86.2$ ($r = 0.995$), 90% Acetone–water, S_N1 : $\Delta G^\ddagger = 26.1\sigma^+ + 95.6$ ($r = 0.998$), $\Delta H^\ddagger = 17.3\sigma^+ + 79.5$ ($r = 0.949$), $\Delta S^\ddagger = -29.5\sigma^+ - 54.0$ ($r = 0.568$). Data measured in methanol and 90% acetone–water mixtures are not plotted in the figure.]

mechanism of the reaction and on the solvent (Table 2, refer to data given in caption of Fig. 3). Very similar slope for the ΔG^\ddagger versus σ^+ plot ($\delta\Delta G^\ddagger = 25.9\text{ kJ mol}^{-1}$) was calculated by DiLabio and Ingold^[22] for the hydrolysis of cumyl chlorides in water.

Entropies of activation computed for both mechanisms are positive (Table 2, $\Delta S^\ddagger \approx 35\text{ J mol}^{-1}\text{ K}^{-1}$) and proved to be independent of the X substituents; therefore, the slopes of the calculated ΔG^\ddagger versus σ^+ and ΔH^\ddagger versus σ^+ plots are almost equal in ethanol ($\delta\Delta G^\ddagger \sim \delta\Delta H^\ddagger$, $\delta\Delta S^\ddagger \sim 0$, Fig. 3). On the other hand, negative entropy of activation values were measured^[16] in 90% acetone–water solvent mixture ($\Delta S^\ddagger = -54\text{ J mol}^{-1}\text{ K}^{-1}$ for the reaction $7a \rightleftharpoons TS 8a$, Table 2, Fig. 3) because charges formed in the TS need solvation. The difference of the computed and measured entropy of activation data can be another reason of the difference of the computed and measured ΔG^\ddagger values.

The results of computations support that solvolysis of cumyl chlorides proceed with S_N1 mechanism for compounds bearing e-d groups, and with S_N2 (intermediate) mechanism for derivatives having e-w substituents. However, in accordance with results of former studies,^[21] the nucleophilic assistance of the water molecules in the S_N2 (intermediate) process is weak, it decreases markedly with the decreasing e-w effect of the substituents (Fig. 2), and does not influence the substituent effect significantly (Fig. 3). The $\delta\Delta G^\ddagger$ values can be calculated with good approximation for both mechanisms of the reaction. The calculated charges and bond distances of TSs **8** and **9** similar to those of TSs **3** and **4** of the hydrolysis of *tert*-butyl chloride, respectively (Table 1).

Hydrolysis of benzyl chlorides

The mechanism of the hydrolysis of benzyl chlorides (**10**) was supposed to change with the substituents of the benzene ring. Kohnstam^[23] has presented evidences that benzyl chlorides, substituted with strongly e-d 4-MeO or 4-PhO groups react by the S_N1 mechanism (Scheme 2, $10 \rightleftharpoons TS 11$), while those substrates which bear alkyl or e-w groups hydrolyze by the S_N2 mechanism ($10 + 2 \rightleftharpoons TS 12$). On the other hand, Friedberger and Thornton,^[24] besides McLennan^[25] came to the conclusion that loose and tight S_N2 TSs are more consistent with the observed kinetic isotope effect data, even in the case of the 4-MeO substituted derivative. Moreover, simultaneous or borderline S_N1 - S_N2 mechanisms,^[26,27] and the participation of ion-pair intermediates^[28,29] have also been proposed for the hydrolysis of benzyl chlorides bearing e-d groups.

We have performed DFT calculations on the reactants and TSs of the S_N1 and S_N2 hydrolyses (Scheme 2) of several ring-substituted benzyl chlorides in water, at 298 K. Parameters of the optimized structures and thermochemical data are listed in Tables 1 and 2 moreover in Tables S3, S4, S7, and S8 in the Supplementary Material. The calculated activation parameters for S_N1 and S_N2 reactions have been compared with the data obtained from the first- (k_1) and second ($k_2 = k_1/[H_2O]$)-order rate constants, respectively, measured in water^[30] and in 50 and 70% acetone–water mixtures.^[23,27,31]

Scans have been made to calculate the structure of TSs **11** of the S_N1 hydrolysis of benzyl chlorides (**10**) at the (B3LYP)/6-31G(d) level, increasing the Cl–C⁷ distance stepwise. The obtained optimized structures of minimum energy have only one imaginary frequency, which is the stretching vibration of the Cl–C⁷ bond. The calculated $\Delta E^\ddagger/\Delta G^\ddagger/\Delta H^\ddagger/\Delta S^\ddagger$ versus $R(\text{ClC}^7)$ plots for TS **11a** of the reaction of benzyl chloride (**10a**) are given in Fig. 1. Only the ΔG^\ddagger data have a maximum at 3.68 Å, where ΔS^\ddagger begins to increase steeply. This structure with maximum value of ΔG^\ddagger can be regarded as TS **11a** of the S_N1 reaction.

In TSs **11** the net Mulliken charges of chlorine is approximately –0.94 a.u., the Cl–C⁷ bond is perpendicular to the aromatic ring [$\varphi(\text{ClC}^7\text{C}^1\text{C}^2) \sim 90^\circ$], the H⁸ and H^{8'} atoms are coplanar with the benzene ring [$\varphi(\text{H}^8\text{C}^7\text{C}^1\text{C}^2) \sim -179^\circ$, $\varphi(\text{H}^{8'}\text{C}^7\text{C}^1\text{C}^2) \sim -0.5^\circ$]. These data do not depend on the X substituent of the aromatic ring significantly; only the Q(Cl) charges of 4-MeO and 4-NO₂ derivatives are slightly different (–0.928 a.u.). On the other hand, the $R(\text{ClC}^7)$ distances increase, the $\theta(\text{ClC}^7\text{C}^1)$ angles decrease (Table 1), the TSs become looser with the increasing e-w effect and σ^+ constant of the X groups [$R(\text{ClC}^7) = 0.28\sigma^+ + 3.66$ ($r = 0.981$); $\theta(\text{ClC}^7\text{C}^1) = -3.27\sigma^+ + 117$ ($r = 0.919$)].

The optimized structures for the S_N2 TSs (**12**) of the hydrolysis of benzyl chlorides (**10**) can be calculated at the (B3LYP)/6-31G(d) level with one imaginary frequency for compounds bearing substituents from 4-NO₂ to 4-Me groups. The calculations on TS of the 4-MeO derivative (**12b**) resulted in two imaginary frequencies because water is bonded much looser to the C⁷ atom in this case. TSs **12** have distorted trigonal bipyramidal (TBP) geometry [$\theta(\text{ClC}^7\text{O}) \sim 160^\circ$]. The Q(Cl) negative charge, the $R(\text{ClC}^7)$ and $R(\text{OC}^7)$ distances as well as the $\theta(\text{ClC}^7\text{C}^1)$ and $\theta(\text{OC}^7\text{C}^1)$ bond angles increase, whereas the Q(O) positive charge and the $\theta(\text{ClC}^7\text{O})$ bond angle decrease with the decrease in the σ^+ constants of the X substituents (Figs. 4 and S1). Thus, with the increasing e-d effect of the substituents, both the leaving group and the nucleophile move away from the C⁷ atom and from the benzene ring. Loose and tight TSs are formed with more

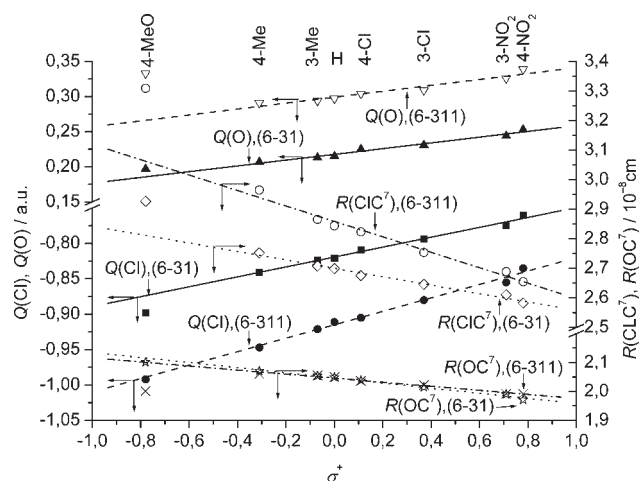
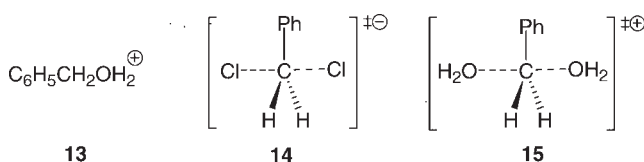


Figure 4. Plots of the $Q(Cl)$ and $Q(O)$ charges and $R(ClC^7)$ and $R(OC^7)$ distances of TSs **12** against the σ^+ substituent constants for the reactions $XC_6H_4CH_2Cl + H_2O \rightleftharpoons TS \ b{12}$, (Scheme 2) calculated at (B3LYP)/6-31G(d) and (B3LYP)/6-311+G(d,p) levels, in water, at 298 K. [Correlations, (B3LYP)/6-31G(d) level: $Q(Cl) = 0.070\sigma^+ - 0.819$ ($r = 0.994$), $Q(O) = 0.041\sigma^+ + 0.218$ ($r = 0.987$), $R(ClC^7) = -0.142\sigma^+ + 2.700$ ($r = 0.992$), $R(OC^7) = -0.088\sigma^+ + 2.047$ ($r = 0.994$); (B3LYP)/6-311+G(d,p) level: $Q(Cl) = 0.095\sigma^+ - 0.915$ ($r = 0.994$), $Q(O) = 0.042\sigma^+ + 0.299$ ($r = 0.967$), $R(ClC^7) = -0.261\sigma^+ + 2.859$ ($r = 0.990$), $R(OC^7) = -0.070\sigma^+ + 2.045$ ($r = 0.989$). The data of the 4-MeO derivative (TS **12b**) were omitted from the correlations.]

and less distorted TBP geometry in the presence of e-d and e-w substituents, respectively. Structural parameters give linear correlations with the σ^+ substituent constants (Figs. 4 and S1) because e-d through-conjugation exists between the X substituents of the aromatic ring and the reaction center. The plane of the $Cl\cdots C^7\cdots O$ atoms is perpendicular to that of the benzene ring [$\varphi(ClC^7C^1C^2) \sim 90^\circ$, $\varphi(OC^7C^1C^2) \sim -90^\circ$]. Even more polar and looser structures with greater negative $Q(Cl)$ and positive $Q(O)$ charges, $R(ClC^7)$ distances as well as $\theta(OC^7C^1)$ and $\theta(ClC^7C^1)$ bond angles were obtained for the calculations performed at the higher (B3LYP)/6-311+G(d,p) level (Figs. 4 and S1, Table S4).

Late TS **12a** is formed in the S_N2 reactions of benzyl chloride because water is a poor nucleophile. The hydrogen atoms of the CH_2 group are bent towards the chlorine [$\varphi(H^8C^7C^1C^2) \sim 173^\circ$, $\varphi(H^8C^7C^1C^2) \sim 5.7^\circ$]. By use of the calculated $C-Cl$ and $C-O$ bond distances (R_o) of benzyl chloride (**10a**; 1.864 Å) and protonated benzyl alcohol (**13**; 1.545 Å), furthermore the distances of $Cl\cdots C^7$ and $O\cdots C^7$ bonds (R) in the symmetric ($n = 0.5$) TSs **14** (2.182 Å), and **15** (2.565 Å) and in TS **12a** of the hydrolysis (2.699 and 2.049 Å), the bond orders $n = 0.44$ and 0.58 were calculated for $Cl\cdots C^7$ and $O\cdots C^7$ bonds of TS **12a**, respectively, with the Pauling equation^[32] [$R - R_o = a \ln(n)$. ($a = -0.920$ and -1.011 were calculated for the $Cl\cdots C^7$ and $O\cdots C^7$ bonds, respectively.)



Free energies of activation, computed for the S_N2 reactions in water (**10 + 2** \rightleftharpoons TS **12**), give linear correlations with the σ^+ constants (Fig. 5), and e-d effect of substituents accelerate the

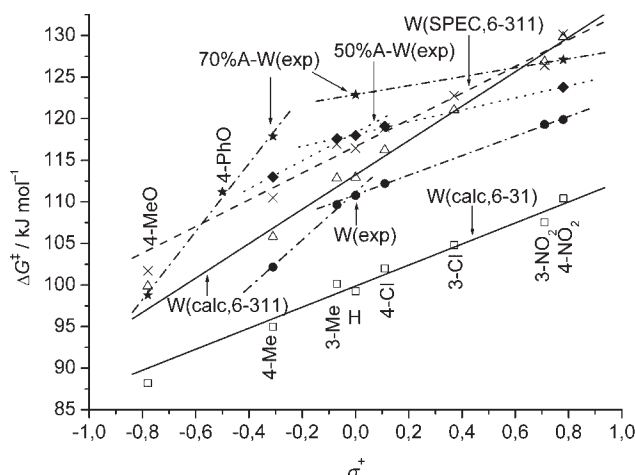


Figure 5. ΔG^\ddagger versus σ^+ plots for the S_N2 hydrolysis of $XC_6H_4CH_2Cl + H_2O \rightleftharpoons TS \ b{12}$ (Scheme 1 $T = 298$ K). Computations were performed in water (W) at (B3LYP)/6-31G(d) and (B3LYP)/6-311+G(d,p) levels with optimization and with SPEC. Experimental data were calculated from the second-order rate constants ($k_2 = k_1/[H_2O]$) measured in water^[30] (W) and in 50 and 70 v/v% acetone–water (A-W) mixtures.^[23,27,31] [Correlations: W(calc, 6-31), $\Delta G^\ddagger = 12.7\sigma^+ + 99.9$ ($r = 0.983$); W(calc, 6-311), $\Delta G^\ddagger = 20.7\sigma^+ + 113$ ($r = 0.995$); W(SPEC, 6-311), $\Delta G^\ddagger = 16.0\sigma^+ + 117$ ($r = 0.986$); W(exp), for $\sigma^+ \geq 0$, $\Delta G^\ddagger = 11.8\sigma^+ + 111$ ($r = 1.000$), for $\sigma^+ \leq 0$, $\Delta G^\ddagger = 28.6\sigma^+ + 111$ ($r = 0.995$); 50% A-W(exp), for $\sigma^+ \geq 0$, $\Delta G^\ddagger = 7.20\sigma^+ + 118$ ($r = 0.999$), for $\sigma^+ \leq 0$, $\Delta G^\ddagger = 17.2\sigma^+ + 118$ ($r = 0.992$); 70% A-W(exp), for $\sigma^+ \geq 0$, $\Delta G^\ddagger = 5.38\sigma^+ + 123$, for $\sigma^+ \leq -0.31$, $\Delta G^\ddagger = 40.9\sigma^+ + 131$. The data of the 4-MeO derivative (TS **12b**) were omitted from the correlations of W(calc, 6-31), W(calc, 6-311) and W(SPEC, 6-311).]

reaction ($\delta\Delta G^\ddagger > 0$). The ΔG^\ddagger values computed at (B3LYP)/6-31G(d) level are lower, while those obtained at the (B3LYP)/6-311+G(d,p) level are higher than the experimental data, measured in water. The ΔG^\ddagger values obtained by single point energy calculations (SPEC) deviate from the results computed with optimization at (B3LYP)/6-311+G(d,p) level for compounds with e-d groups, which have looser TSs (Fig. 5). In accordance with earlier observations on the reaction of benzyl halides with nucleophiles,^[5b,33–35] experimentally derived^[23,27,30,31] ΔG^\ddagger versus σ^+ plots show breaks at $\sigma^+ \sim 0$ (Fig. 5). The reactivity of the derivatives with e-w groups are higher than expected from a linear correlation (Fig. 5). Earlier this type of breaks of the Hammett plots were explained with the change of the mechanism of the reactions.^[36] We found, however, that in the S_N2 nucleophilic substitutions of benzyl halides broken ΔG^\ddagger versus σ^+ plots at $\sigma^+ \sim 0$ can also be obtained when the structure of the TSs is changed with the substituents.^[5b] Therefore, the break of the ΔG^\ddagger versus σ^+ plots at $\sigma^+ < 0$ of the hydrolysis of benzyl chlorides with strong e-d groups can be explained with the change of the mechanism from S_N2 to S_N1 , but for the break at $\sigma^+ \sim 0$ on the plots of compounds with alkyl and e-w substituents, the change of the structure of the TS seems to be a better interpretation.

The ΔS^\ddagger and ΔH^\ddagger parameters, calculated for the S_N2 hydrolysis of benzyl chlorides show great deviations from the experimentally derived data^[30,31] (Table 2) because the latter are influenced by the rearrangement of the solvent molecules, which cannot be computed with the applied methods. Experimentally derived $\Delta S^\ddagger/\Delta H^\ddagger$ versus σ^+ plots (Fig. S2) are also broken at $\sigma^+ \sim 0$, which may refer to a change of solvation with the substituents, too. ΔS^\ddagger data, calculated from kinetic measurements, increase with the

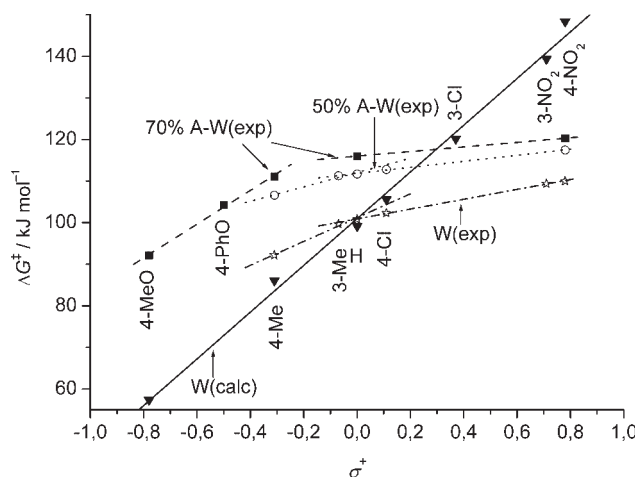


Figure 6. Calculated and experimentally derived ΔG^\ddagger versus σ^+ plots for the S_N1 hydrolysis of $XC_6H_4CH_2Cl \rightleftharpoons TS 11$ (Scheme 1 $T = 298$ K). Computations were performed at (B3LYP)/6-31G(d) level in water (W). Experimental data were calculated from the first-order rate constants, measured in water^[30] (W) and in 50 and 70 v/v% acetone–water (A–W) mixtures^[23,27,31] [Correlations: W(calc), $\Delta G^\ddagger = 56.2\sigma^+ + 99.2$ ($r = 0.997$); W(exp), for $\sigma^+ \geq 0$, $\Delta G^\ddagger = 11.8\sigma^+ + 101$ ($r = 1.000$), for $\sigma^+ \leq 0$, $\Delta G^\ddagger = 28.6\sigma^+ + 101$ ($r = 0.995$); 50%A–W(exp), for $\sigma^+ \geq 0$, $\Delta G^\ddagger = 7.20\sigma^+ + 112$ ($r = 0.999$), for $\sigma^+ \leq 0$, $\Delta G^\ddagger = 17.2\sigma^+ + 112$ ($r = 0.992$); 70%A–W(exp), for $\sigma^+ \geq 0$, $\Delta G^\ddagger = 5.38\sigma^+ + 116$, for $\sigma^+ \leq -0.31$, " $> \times + < \Delta G^\ddagger = \div$ " " $\sigma^+ + - - - >$ "

increase in polarity and solvation of the TSs because water molecules are less ordered in the solvent shell of the TSs than in the bulk of the solvent.^[5,6] The measured ΔH^\ddagger parameters^[5a] are influenced by the contribution originating from ΔS^\ddagger .

Free energies of activation, computed at the (B3LYP)/6-31G(d) level for the S_N1 reaction (**10** \rightleftharpoons **TS 11**) in water, give linear correlations against the σ^+ constants (Fig. 6). The slopes of the computed ΔG^\ddagger versus σ^+ plots are much greater for the S_N1 than for S_N2 reaction (Table 2), similar change of reactivity with the substituents has been measured only in the reaction of the 4-MeO and 4-PhO derivatives in 70% acetone–water solvent (Figs. 5 and 6). In water the experimentally derived ΔG^\ddagger values of compounds with e-w substituents are smaller than the computed data, indicating that the reaction of these derivatives proceed with S_N2 mechanism.

CONCLUSIONS

In S_N1 reactions the total energy increases continuously with the increase in the distance of the splitting bond, while free energy activation, which determines the rate of the reaction, may have a maximum value when entropy of activation increases. The optimized structure of the S_N1 TSs can be calculated therefore via relaxed scan applied to the bond of the leaving group.

Free energy of activation is influenced the least by solvent rearrangement among activation parameters, and the mechanism of the solvolytic reactions can be investigated by studying the effect of substituents on this parameter. Experimentally derived ΔH^\ddagger and ΔS^\ddagger parameters are influenced markedly by the rearrangement of solvent therefore they do not agree with the calculated data. The error of ΔG^\ddagger originating from a second imaginary frequency of the TS can be corrected by including a

cluster of water molecules into the reactants, having the same imaginary frequency as the TS.

The mechanism of the solvolytic reactions of benzyl chlorides and cumyl chlorides changes with the steric hindrance and with the electronic effects of substituents of the aromatic ring. In the case of benzyl chlorides the structures of the S_N2 TSs change with the substituents, loose and tight TSs are formed for substrates bearing alkyl and e-w groups, respectively. The polarity of the TSs increases with the increasing e-d effect of the substituents. Polar TSs are stabilized by the solvent and this is the reason why e-d effect of substituents of the benzene ring accelerates an S_N2 reaction. The hydrolysis of benzyl chlorides, substituted with a strong e-d group (e.g., 4-MeO) proceeds with an S_N1 mechanism in protic solvent, and the nucleophilic assistance of the solvent has only minor importance. The distances of the nucleophile and the leaving group from the center of the reaction are much greater in hydrolyses of cumyl chlorides with great steric hindrance. Nucleophilic assistance occurs only in reactions of derivatives with e-w groups, but this does not influence reactivity markedly.

COMPUTATIONAL METHODS

The geometry of the compounds was fully optimized without symmetry constraints by use of the Gaussian 03 software package^[37] at the DFT(B3LYP)/6-31G(d) level in solvents, at 298 K. In the case of benzyl chlorides, geometry optimizations and SPEC were also performed at the more extended DFT(B3LYP)/6-311+G(d,p) level. Scans were made increasing the Cl–C distance stepwise, to calculate the optimized structures of TSs of the S_N1 solvolyses of *tert*-butyl chloride, cumyl chlorides, and benzyl chlorides. The solvent effect was incorporated by application of the PCM^[38] in the integral equation formalism^[39,40] (IEF-PCM) of the corresponding solvent, i.e., calculations were performed in a polarizable, continuous medium of the same dielectric constant as the solvent. All structures were characterized as energy minima or TSs by calculation of the harmonic vibration frequencies, with use of analytical second derivatives. No or one imaginary frequency was obtained for reactants and TSs, respectively, except the cases of some loose structures, bearing a very weakly bonded water molecule. Selected data for the optimized structures obtained by means of DFT calculations and the number of imaginary frequencies are listed in Tables S1–S4 and Tables S5–S8 in the Supplementary Material, respectively.

The efficiency of methods used for exploring potential energy surfaces may decrease when applied with solvent models since their potential energy surface is less smooth than one can expect for regular quantum chemical methods in gas phase. This effect may result in additional imaginary vibrational frequencies, which can be regarded as numerical errors but they also cause an extra effect by preventing the inclusion of the corresponding normal modes in the thermochemical analysis. Instead of excluding such data from our study we applied a workaround to the problem by exploiting the fact that only differences of thermochemical data were utilized. When such problem of extra imaginary frequencies occurred at one side of a reaction than we expanded the equations to reproduce the extra imaginary frequencies also in the other side of the reaction. In TSs **4** and **8** the extra imaginary frequency belongs to the libration of the very weakly bonded water molecule. We have created a cluster of three water

molecules, where one of the water molecules is in similar situation as in the given TSs and also produces an extra imaginary frequency. The effect of the extra imaginary frequencies vanishes when we add a cluster of two water molecules (with no imaginary frequency) to the TS side of the equation and the cluster of three water molecules (with one imaginary frequency) to the reactant side. If the IFC was used in similar fashion it has been indicated in the text.

The sums of the electronic and thermal free energies (G) and enthalpies (H) and also the entropies of formation (S) for reactants and TSs were obtained by the standard procedure in the framework of the harmonic approximation,^[41,42] and are listed together with the calculated total energies (E) in Tables S5–S8 in the Supplementary Material. The computed entropy (S) values obtained in solutions agree with the data measured in the gas-phase or calculated by application of Benson's rule.^[43] As examples, the S values of 194.9, 243.6, 356.2, and 399.2 J mol⁻¹ K⁻¹ were obtained for H₂O, CH₃Cl, C₆H₅CH₂Cl, and C₆H₅CMe₂Cl with DFT calculations in solutions, respectively. In comparison, the values of S = 188.8 and 234.6 J mol⁻¹ K⁻¹ were measured for H₂O and CH₃Cl in the gas-phase,^[44] and S = 355.7 and 411.1 J mol⁻¹ K⁻¹ were calculated for C₆H₅CH₂Cl and C₆H₅CMe₂Cl at 25°C on application of Benson's rule, respectively. The ΔE^\ddagger , ΔG^\ddagger , ΔH^\ddagger , ΔS^\ddagger parameters for the reactions were calculated from the differences in the E , G , H , and S values of the TSs and reactants, respectively. The generated ΔE^\ddagger , ΔG^\ddagger , and ΔH^\ddagger values were multiplied by 627.51 and 4.184 in order to convert them into kJ mol⁻¹ units. Experimentally derived activation parameters for S_N1 and S_N2 reactions were calculated from the first-order (k_1) and second-order ($k_2 = k_1/[H_2O]$) rate constants, respectively. The $\delta\Delta G^\ddagger$, $\delta\Delta H^\ddagger$, and $\delta\Delta S^\ddagger$ reaction constants were calculated from the activation parameters obtained through the DFT computations and from kinetic measurements, by using Eqn 1 with the σ^+ substituent constants,^[45] as described previously.^[5,6] The $\Delta G^\ddagger/\Delta H^\ddagger/\Delta S^\ddagger$ versus σ^+ plots of the reactions of benzyl substrates often have two linear components, separately for compounds with e-w and e-d substituents, with a break at $\sigma^+ \approx 0$. The data for the unsubstituted compound seem to belong to both lines. In these cases, the $\delta\Delta G^\ddagger$, $\delta\Delta H^\ddagger$, and $\delta\Delta S^\ddagger$ reaction constants were calculated by use of Eqn 1, separately for compounds bearing e-w and e-d substituents.

SUPPLEMENTARY MATERIAL

Optimized bond lengths, atomic charges, bond angles, torsion angles, calculated total energies, sums of electronic and thermal free energies and enthalpies, entropies of formation, and number of imaginary frequencies are listed in the Supplementary Material, available in Wiley-Interscience.

Acknowledgements

This work was supported by the Hungarian Scientific Research Foundation and GVOP (OTKA no. K 60889 and GVOP-3.1.1.-2004-05-0451/3.0).

REFERENCES

[1] a) C. K. Ingold, *Structure and Mechanism in Organic Chemistry*, 2nd ed., Bell, London, 1969; b) S. R. Hartshorn, *Aliphatic Nucleophilic Substitution*, Cambridge University Press, Cambridge, 1973; c) A. R. Katritzky,

B. E. Brycki, *Chem. Soc. Rev.* **1990**, 19, 83–105; d) S. S. Shaik, H. Schlegel, S. Wolfe, *Theoretical Aspects of Physical Organic Chemistry. The S_N2 Mechanism*, Wiley, New York, 1992; e) J.-L. M. Abboud, R. Notario, J. Bertran, M. Sola, *Prog. Phys. Org. Chem.* **1993**, 19, 1–182, and references therein; f) M. B. Smith, J. March, *March's Advanced Organic Chemistry, Reactions, Mechanism, and Structure*, 5th ed., Wiley, New York, 2001. pp. 381–462, and references therein.

[2] a) H. Kim, J. T. A. Hynes, *J. Am. Chem. Soc.* **1992**, 114, 10508–10528; b) J. R. Mathis, H. Kim, J. T. A. Hynes, *J. Am. Chem. Soc.* **1993**, 115, 8248–8262; c) J. P. Richard, T. L. Amyes, M. M. Toteva, *Acc. Chem. Res.* **2001**, 34, 981–988; d) S. Minegishi, R. Loos, S. Kobayashi, H. Mayr, *J. Am. Chem. Soc.* **2005**, 114, 2641–2649; e) K. S. Peters, *Acc. Chem. Res.* **2007**, 40, 1–7.

[3] a) T. W. Bentley, P. R. Schleyer, *J. Am. Chem. Soc.* **1976**, 98, 7658–7666; b) F. L. Schadt, T. W. Bentley, P. R. Schleyer, *J. Am. Chem. Soc.* **1976**, 98, 7667–7674; c) T. W. Bentley, C. T. Bowen, D. H. Morten, P. R. Schleyer, *J. Am. Chem. Soc.* **1981**, 103, 5466–5475; d) T. W. Bentley, G. E. Carter, *J. Am. Chem. Soc.* **1982**, 104, 5741–5747; e) T. W. Bentley, C. T. Bowen, W. Parker, C. I. F. Watt, *J. Am. Chem. Soc.* **1979**, 101, 2486–2488; f) T. W. Bentley, C. T. Bowen, W. Parker, C. I. F. Watt, *J. Chem. Soc., Perkin Trans. 2* **1980**, 1244–1252.

[4] J. J. Gajewski, *J. Am. Chem. Soc.* **2001**, 123, 10877–10883.

[5] a) F. Ruff, Ö. Farkas, *J. Org. Chem.* **2006**, 71, 3409–3416; b) F. Ruff, Ö. Farkas, A. Kucsman, *Eur. J. Org. Chem.* **2006**, 5570–5580.

[6] a) F. Ruff, *J. Mol. Struct. (Theochem.)* **2002**, 617, 31–45; b) F. Ruff, *Internet Electron. J. Mol. Des.* **2004**, 3, 474–498. <http://www.biochempress.com>

[7] a) L. G. Hepler, W. F. O'Hara, *J. Phys. Chem.* **1961**, 65, 811–814; b) L. G. Hepler, *J. Am. Chem. Soc.* **1963**, 85, 3089–3092; c) J. W. Larson, L. G. Hepler, *J. Org. Chem.* **1968**, 33, 3961–3963; d) L. G. Hepler, *Can. J. Chem.* **1971**, 49, 2803–2807; e) T. Matsui, L. G. Hepler, *Can. J. Chem.* **1977**, 54, 1296–1299.

[8] a) W. P. Keirstead, K. R. Wilson, J. T. Hynes, *J. Chem. Phys.* **1991**, 95, 5256–5257; b) R. M. C. Goncalves, A. M. N. Simoes, L. M. P. C. Albuquerque, E. A. Macedo, *J. Phys. Org. Chem.* **1993**, 6, 133–138; c) D. S. Hartsough, K. M. Merz, *J. Phys. Chem.* **1995**, 99, 384–390; d) E. D. German, A. M. Kuznetsov, V. A. Tikhomirov, *J. Electroanal. Chem.* **1997**, 420, 235–241; e) D. D. Sung, J.-Y. Kim, I. Lee, S. S. Chung, K. H. Park, *Chem. Phys. Lett.* **2004**, 392, 378–382.

[9] S. Yamabe, E. Yamabe, T. Minato, *J. Chem. Soc., Perkin Trans. 2* **1983**, 1881–1884.

[10] M. M. Toteva, J. P. Richard, *J. Am. Chem. Soc.* **1996**, 118, 11434–11445.

[11] a) A. H. Fainberg, S. Winstein, *J. Am. Chem. Soc.* **1956**, 78, 2770–2777; b) S. Winstein, A. H. Fainberg, *J. Am. Chem. Soc.* **1957**, 79, 5937–5950.

[12] W. L. Jorgensen, J. K. Bucker, S. E. Huston, P. J. Rossky, *J. Am. Chem. Soc.* **1987**, 109, 1891–1899.

[13] A. G. Martinez, E. T. Vilar, J. O. Barcina, S. D. Cerero, *J. Org. Chem.* **2005**, 70, 10238–10246.

[14] a) H. Yamataka, M. Aida, *Chem. Phys. Lett.* **1998**, 289, 105–109; b) M. Aida, H. Yamataka, M. Dupuis, *Chem. Phys. Lett.* **1998**, 292, 474–480; c) M. Aida, H. Yamataka, M. Dupuis, *Theor. Chem. Acc.* **1999**, 102, 262–271; d) M. Aida, H. Yamataka, *J. Mol. Struct. Theochem.* **1999**, 461, 417–427.

[15] M. H. Abraham, D. J. McLennan, *J. Chem. Soc., Perkin Trans. 2* **1977**, 873–879.

[16] a) H. C. Brown, J. D. Brady, M. Grayson, W. H. Bonner, *J. Am. Chem. Soc.* **1957**, 79, 1897–1903; b) H. C. Brown, Y. Okamoto, G. Ham, *J. Am. Chem. Soc.* **1957**, 79, 1906–1909; c) Y. Okamoto, T. Inukai, H. C. Brown, *J. Am. Chem. Soc.* **1958**, 80, 4979–4987.

[17] a) H. J. Koh, H. W. Lee, I. Lee, *J. Chem. Soc., Perkin Trans. 2* **1994**, 125–129; b) I. Lee, H. J. Koh, S. N. Hong, B. S. Lee, *Gazz. Chim. Ital.* **1995**, 125, 347–351; c) S. Balachandran, R. S. Devi, D. S. Kumar, *Asian J. Chem.* **2005**, 17, 1216–1220.

[18] a) K.-T. Liu, L.-W. Chang, P.-S. Chen, *J. Org. Chem.* **1992**, 57, 4791–4793; b) K.-T. Liu, P.-S. Chen, P.-F. Chiu, M.-L. Tsao, *Tetrahedron Lett.* **1992**, 33, 6499–6502.

[19] a) V. A. Amelichev, G. V. Saidov, *Zh. Obsh. Khim.* **1981**, 51, 187–192; b) V. A. Amelichev, G. V. Saidov, *Zh. Obsh. Khim.* **1981**, 51, 1874–1879; c) V. A. Amelichev, M. V. Nosovskii, G. V. Saidov, *Zh. Obsh. Khim.* **1981**, 51, 1879–1885.

[20] D. N. Kevill, M. J. Dsouza, *J. Chem. Res. -S.* **1993**, 332–333.

[21] a) J. P. Richard, T. L. Amyes, T. Vontor, *J. Am. Chem. Soc.* **1991**, 113, 5871–5873; b) J. P. Richard, V. Jagannadham, T. L. Amyes, M. Mishima, Y. Tsuno, *J. Am. Chem. Soc.* **1994**, 116, 6706–6712.

[22] G. A. DiLabio, K. U. Ingold, *J. Org. Chem.* **2004**, 69, 1620–1624.

[23] a) G. Kohnstam, *Adv. Phys. Org. Chem.* **1967**, *5*, 121–169, and references therein; b) B. J. Gregory, G. Kohnstam, A. Queen, D. J. Reed, *Chem. Commun.* **1971**, 797–799.

[24] M. P. Friedberger, E. R. Thornton, *J. Am. Chem. Soc.* **1976**, *98*, 2861–2865.

[25] D. J. McLennan, *Acc. Chem. Res.* **1976**, *9*, 281–287.

[26] J. M. Harris, *Prog. Phys. Org. Chem.* **1974**, *11*, 89–173.

[27] A. Queen, *Can. J. Chem.* **1979**, *57*, 2646–2657.

[28] R. A. Sneed, *Acc. Chem. Res.* **1973**, *6*, 46–53.

[29] H. Aronovitch, A. Porss, *J. Chem. Soc., Perkin Trans. 2* **1978**, 540–545.

[30] J. B. Hyne, R. Wills, R. E. Wonka, *J. Am. Chem. Soc.* **1962**, *84*, 2914–2919.

[31] a) E. Tommila, E. Paakkala, U. K. Virtanen, A. Erva, S. Vavila, *Ann. Acad. Sci. Fennicae* **1959**, A No. **91**, 3–36; b) E. Tommila, *Acta Chem. Scand.* **1966**, *20*, 923–936.

[32] L. Pauling, *J. Am. Chem. Soc.* **1947**, *69*, 542–553.

[33] R. A. Y. Jones, *Physical and Mechanistic Organic Chemistry*, 2nd ed., Cambridge University Press, Cambridge, **1984**, pp. 155–158, and references contained therein.

[34] T. Thorstenson, R. Eliason, A. Songstad, *Acta Chem. Scand.* **1977**, A*31*, 276–280.

[35] F. P. Ballistreri, E. Maccarone, A. Mamo, *J. Org. Chem.* **1976**, *41*, 3364–3366.

[36] a) O. Exner, in *Advances in Linear Free Energy Relationships* (Eds: N. B. Chapman, J. Shorter), Plenum Press, New York, **1972**, Chap. 1; b) F. Ruff, I. G. Csizmadia, *Organic Reaction, Equilibria, Kinetics and Mechanism*, Elsevier, Amsterdam, **1994**.

[37] M. J. Frisch, G. W. Trucks, H. B. Schlegel, G. E. Scuseria, M. A. Robb, J. R. Cheeseman, J. A. Montgomery, Jr T. Vreven, K. N. Kudin, J. C. Burant, J. M. Millam, S. S. Iyengar, J. Tomasi, V. Barone, B. Mennucci, M. Cossi, G. Scalmani, N. Rega, G. A. Peterson, H. Nakatsuji, M. Hada, M. Ehara, K. Toyota, R. Fukuda, J. Hasegawa, M. Ishida, T. Nakajima, Y. Honda, O. Kitao, H. Nakai, M. Klene, X. Li, J. E. Knox, H. P. Hartchian, J. B. Cross, C. Adamo, C. Jaramillo, R. Gomperts, R. E. Stratmann, O. Yazyev, A. J. Austin, R. Cammi, C. Pomelli, J. W. Ochterski, P. Y. Ayala, K. Morokuma, G. A. Voth, P. Salvador, J. J. Dannenberg, V. G. Zakrzewski, S. Dapprich, A. D. Daniels, M. C. Strain, Ö. Farkas, D. K. Malick, A. D. Rabuck, K. Raghavachari, J. B. Foresman, J. V. Ortiz, Q. Cui, A. G. Baboul, S. Clifford, J. Cioslowski, B. B. Stefanov, G. Liu, A. Liashenko, P. Piskorz, I. Komáromi, R. L. Martin, D. J. Fox, T. Keith, L. A. Al-Laham, C. Y. Peng, A. Nanayakkara, M. Challacombe, P. M. W. Gill, B. Johnson, W. Chen, M. W. Wong, C. Gonzalez, J. A. Pople, *Gaussian 03, Revision C.02*, Gaussian, Inc., Pittsburg, PA, **2003**.

[38] J. Tomasi, M. Persico, *Chem. Rev.* **1994**, *94*, 2027–2094.

[39] E. Cancès, B. Mennucci, *J. Chem. Phys.* **2001**, *114*, 4744–4745.

[40] D. M. Chipman, *J. Chem. Phys.* **2000**, *112*, 5558–5565.

[41] D. A. McQuarrie, J. D. Simon, *Molecular Thermodynamics*, University Science Books, Sausalito, CA, **1999**.

[42] http://www.gaussian.com/g_whitepap/thermo/thermo.pdf

[43] a) S. W. Benson, F. R. Cruickshank, D. M. Golden, G. R. Haugen, H. E. O'Neal, A. S. Rodgers, R. Shaw, R. Walsh, *Chem. Rev.* **1969**, *69*, 279–290; b) S. W. Benson, *Thermochemical Kinetics*, Wiley, New York, pp. 19–72.

[44] *CRC Handbook of Chemistry and Physics* (Ed.: D. R. Lide), CRC Press, Boca Roton, **1995**, Chap. 5-4.

[45] C. Hansch, H. Leo, R. W. Taft, *Chem. Rev.* **1991**, *91*, 165–195.